

Electronic Supplementary Material

Crystal facet-dependent CO₂ cycloaddition to epoxides over ZnO catalysts

Yongjian Wei^{1,2}, Ying Li (✉)^{1,2}, Yunfei Xu^{1,2}, Yinghui Sun^{1,2}, Tong Xu^{1,2}, Haiou Liang^{1,2},
Jie Bai^{1,2}

1 Inner Mongolia Key Laboratory of Industrial Catalysis, Hohhot 010051, China

2 College of Chemical Engineering, Inner Mongolia University of Technology, Hohhot 010051, China

E-mail: liying_2021@imut.edu.cn

1 Experimental section

1.1 Characterize

The crystalline properties and crystal structure of the catalysts were characterized using an X-ray diffraction analyzer (XRD, BrukerAXS, Japan) with a sample sweep rate of 10 °/min and a scanning range of 20 °-70 °. The skeletal structure of the samples was determined by Fourier transform infrared spectroscopy (Thermo Nicolet, Nexus 670, USA). The morphological features and microstructures of the catalytic materials were analyzed by field emission scanning electron microscopy (FE-SEM SU8220, Japan) and transmission electron microscopy (TEM, JEOL, Japan). The physical properties of the samples were characterized using the N₂ physical adsorption (BET, Quantachrome Instruments), and the samples were degassed at 200 °C for 12 hours before the test. Specific surface area was calculated using the

Brunauer-Emmett-Teller (BET) algorithm and pore size distribution was calculated using the Barret-Joyner-Halenda (BJH) algorithm. The elemental valence was characterized by X-ray photoelectron spectroscopy (XPS, Thermo Fisher Scientific, USA). The crystal structure and intrinsic defects of the samples were characterized by laser microscopic Raman spectroscopy (Raman, Renishaw in Via microscope) using a laser wavelength of 532 nm, a sweeping range of 200-800 cm^{-1} , an exposure time of 10 s and several scans of 50. The types and concentrations of vacancies were detected by paramagnetic resonance spectrometry (EPR, Bruker EMXplus-6/1, Germany) in the range of 3000-4000 Gauss. The total number of unpaired electron spins in the different vacancies was determined separately by Bruker's absolute quantification method. The weight loss of the reused samples was measured using a thermogravimetric analyzer (TG, Rigaku Therma plus, Japan) at a range of 50 °C to 400 °C with a heating rate of 3 °C /min. The temperature-programmed desorption of CO_2 was measured by a Chemisorption Analyzer (CO_2 -TPD, ChemiMaster 8320, China). First, 0.2g of sample was treated in He at 400 °C for 1 h. Then, CO_2 was adsorbed at 80 °C for 1 h. After purging with He for 1 h to remove the gas phase and physisorbed CO_2 , the temperature was increased to 400 °C at the rate of 10 °C \cdot min⁻¹ for CO_2 desorption. The released CO_2 was recorded by a thermal conductivity detector (TCD).

1.2 Density functional theory (DFT) calculations

Density functional theory (DFT) calculations were carried out using the CASTEP in Materials Studio (MS) software [1]. The Perdew-Burke-Ernzerhof (PBE)

generalized gradient approximation (GGA) functional was used for the exchange-correlation potential [2, 3]. The geometry optimization convergence tolerance of energy and the force were set to 1.0×10^{-5} eV/atom and all atoms were converged to 0.03 eV/Å, respectively. The Brillouin zone was sampled by $3 \times 3 \times 1$ k-point Mon-khorst-Pack grids and an energy cutoff of 450 eV was used.

As shown in Figure S1, the facets of ZnO (002) and ZnO (100) were modeled by a 3×3 unit cell with 8 layers (36 O atoms and 36 Zn atoms) and a 3×2 unit cell with 6 layers (36 O atoms and 36 Zn atoms), respectively. All models have approximately 15 Å of vacuum spacings between the successive metal slabs. The bottom 4 layers of ZnO (002) and bottom 3 layers of ZnO (100) were fixed to their crystal positions. The remaining atoms were relaxed at their bulk-truncated structure.

The O vacancy formation energy calculation formula is as follows:

$$E_f^V = E_V - E_{perf} + E_O$$

Where E_V is the total energy of the system containing one O vacancy, E_{perf} is the total energy of the system without defects, and E_O is the energy of one O atom. The lower E_f^V values indicate that oxygen vacancies are more easily to form on the ZnO surfaces.

The adsorption energy calculation formula is as follows:

$$E_{ads} = E_{A+slab} - E_A - E_{slab}$$

Where E_A is the total energy of the reactant molecule, E_{slab} is the total energy of the surface, and E_{A+slab} is the total energy of surface species on the slab. The lower E_{ads} values indicate that substrates are more easily and stably adsorbed on the

ZnO surfaces.

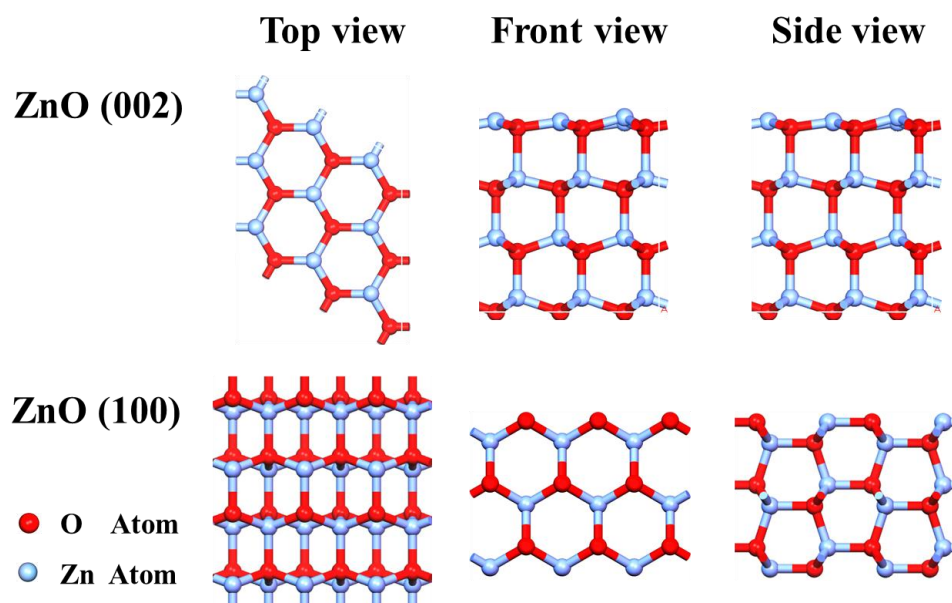


Fig. S1 The models of ZnO (002) and ZnO (100) surfaces

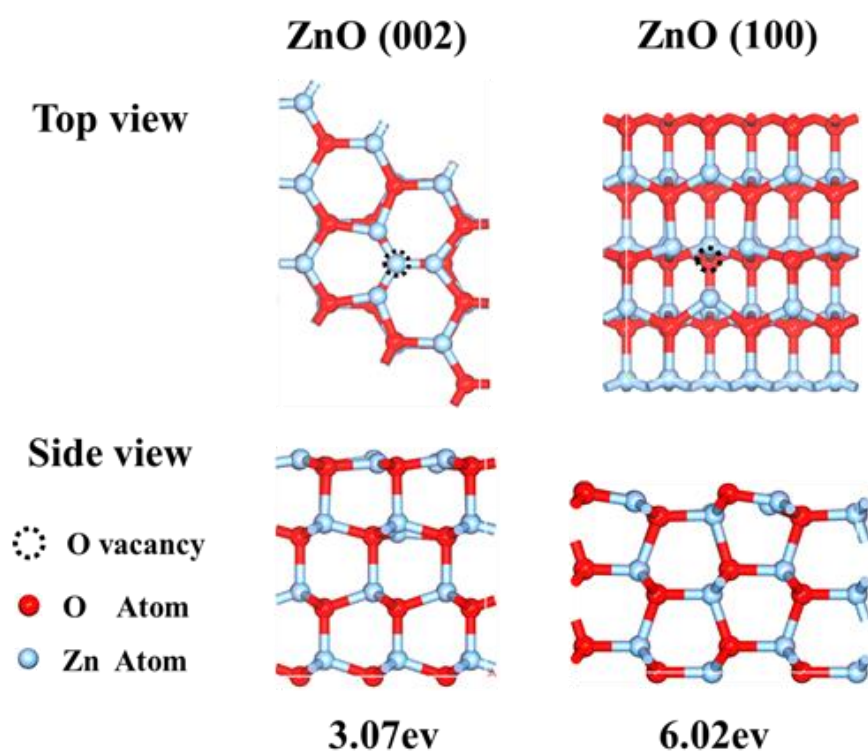


Fig. S2 The formation of oxygen vacancies on the ZnO (002) and ZnO (100) surfaces.

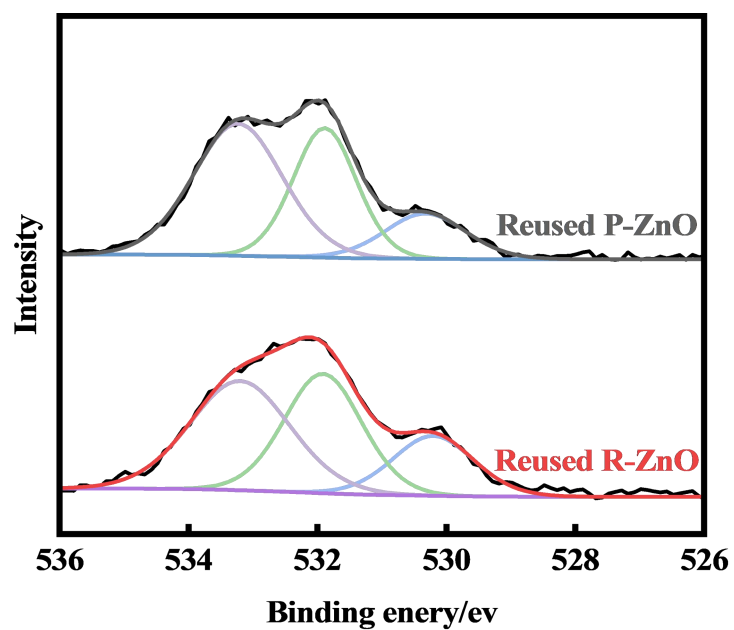


Fig. S3 XPS analysis of O 1S for the reused P-ZnO and R-ZnO.

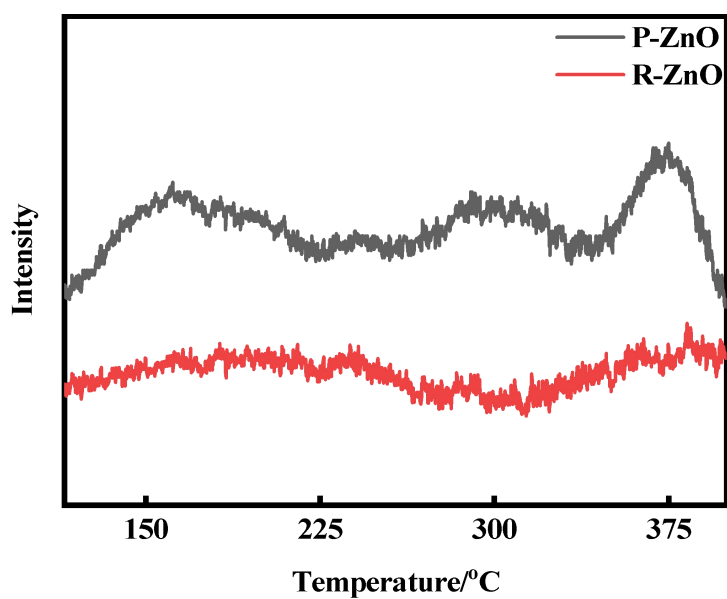


Fig. S4 The CO₂-TPD of P-ZnO and R-ZnO

Table S1 Co-catalytic effect of DMF for the CO₂ cycloaddition reaction.

Entry	Catalyst	Co-catalyst	Selectivity	Yield
1	P-ZnO	none	>99%	4.9%
2	R-ZnO	none	>99%	1.9%
3	none	DMF	>99%	36.9%

4	P-ZnO	DMF	>99%	64.5%
5	R-ZnO	DMF	>99%	42.3%

Reaction conditions: 0.1 g catalysts, 50 μ L DMF, 76.5mmol ECH, 130 $^{\circ}$ C, 2 MPa, 4 h

Table S2 Comparative analysis of the catalytic activity over P-ZnO

Catalyst	ECH dosage /mmol	Reaction conditions	Yield	Reference
Li-MgO	127	130 $^{\circ}$ C, 3 MPa, 4 h, 200 mg catalysts	97.0%	[4]
Mg-Al-Fe metal oxides	34.5	50 $^{\circ}$ C, 0.05 MPa, 7 h, 60 mg catalysts	95.4%	[5]
Mn-Ba metal oxides	30.1	160 $^{\circ}$ C, 2.5 MPa, 6 h, 340 mg catalysts	87.7%	[6]
Ni-Co metal oxides	50	140 $^{\circ}$ C, 3 MPa, 6 h, 92.8 mg catalysts	99.0%	[7]
P-ZnO	76.5	130 $^{\circ}$ C, 1.5 MPa, 4 h, 100 mg catalyst	92.0%	This work

References

- [1] Clark S J S, Matthew D, Pickard, Chris J, Hasnip, Phil J, Probert, Matt I J, Refson, Keith, et al. First principles methods using CASTEP. *Zeitschrift für Kristallographie*, 2005, 220(5-6): 567-570
- [2] Rao G S, Hussain T, Islam M S, Sagynbaeva M, Gupta D, Panigrahi P, Ahuja R. Adsorption mechanism of graphene-like ZnO monolayer towards CO₂ molecules: enhanced CO₂ capture. *Nanotechnology*, 2016, 27(1): 015502
- [3] Xia Y , Pan A F, Su Y Q, Zhao S K, Li Z, Davey A K, Zhao L B, Maboudian R, Carraro C. In-situ synthesized N-doped ZnO for enhanced CO₂ sensing: Experiments and DFT calculations. *Sensors and Actuators B: Chemical*, 2022,

357: 131359

- [4] Rasal K B, Yadav G D, Koskinen R, Keiski R. Solventless synthesis of cyclic carbonates by direct utilization of CO₂ using nanocrystalline lithium promoted magnesia. *Molecular Catalysis*, 2018, 451: 200-208
- [5] Zhang S Q, Wang Q, Puthiaraj P, Ahn W S. MgFeAl layered double hydroxide prepared from recycled industrial solid wastes for CO₂ fixation by cycloaddition to epoxides. *Journal of CO₂ Utilization*, 2019, 34: 395-403
- [6] Kulal N, Vasista V, Shanbhag G V. Identification and tuning of active sites in selected mixed metal oxide catalysts for cyclic carbonate synthesis from epoxides and CO₂. *Journal of CO₂ Utilization*, 2019, 33: 434-444
- [7] Ribeiro S L S, Silva C G, Prado G E T O, da Mata Á F A, Milani J L S, Martins P R, Chagas R P. Nickel–cobalt hydroxide catalysts for the cycloaddition of carbon dioxide to epoxides. *Research on Chemical Intermediates*, 2022, 48(5): 1907-1921